

HER2-Positive Breast Cancer: Tumor-to-Liver SUV Ratio is the Best Parameter for Detection in F-18 FDG-PET/CT

Yoshifumi Noda,¹ Satoshi Goshima,^{1*} Hiroshi Kawada,¹ Nobuyuki Kawai,¹ Hiromi Koyasu,¹ and

Masayuki Matsuo¹

¹Department of Radiology, Gifu University Hospital, Gifu University, Gifu, Japan

*Corresponding author: Satoshi Goshima, M.D., Ph.D, Department of Radiology, Gifu University Hospital, 1-1 Yanagido, Gifu 501-1194, Japan. Tel: +58-2306437, Fax: +58-2306440, E-mail: gossy@par.odn.ne.jp

Received 2016 August 30; Revised 2016 December 13; Accepted 2017 February 03.

Abstract

Background: Fluorine-18 fluorodeoxyglucose (F-18 FDG)-positron emission tomography/computed tomography (PET/CT) is widely used in most malignancy workups, including detection, differential diagnosis, staging and/or restaging, therapeutic decision-making, follow-up, and prognosis.

Objectives: The aim of this study was to evaluate the usefulness of F-18 FDG-PET/CT for predicting breast cancer molecular subtypes.

Patients and Methods: Sixty-six patients with pathologically proven invasive breast carcinoma (IBC) underwent F-18 FDG-PET/CT imaging for tumor staging. The maximum standardized uptake value (tumor SUVmax) of the IBC and mean SUVs of the liver and spleen (liver and spleen SUVmean) were measured. Molecular subtype was determined according to genomic analysis. The tumor SUVmax, tumor-to-liver SUV ratio, and tumor-to-spleen SUV ratio were correlated with molecular subtype data.

Results: Logistic analysis demonstrated that only the tumor-to-liver SUV ratio was a significant parameter for human epidermal growth factor type 2 (HER2)-positive subtype identification ($P = 0.0049$). The sensitivity, specificity, and area under the receiver-operating-characteristic curve (AUC) of this parameter for HER2-positive subtype detection were 83%, 79%, and 0.87, respectively.

Conclusion: The tumor-to-liver SUV ratio appears to be useful for HER2-positive subtype identification, thus indicating the potential use of F-18 FDG-PET/CT as an imaging biomarker that could facilitate the clinical management of patients with breast cancer.

Keywords: Breast Cancer, Positron Emission Tomography, Fluorine 18 Fluorodeoxyglucose, HER2 Gene

1. Background

Molecular subtype classification of breast cancers on the basis of gene expression profiling has proven useful for predicting prognosis, treatment options, and treatment responses (1, 2). However, gene expression profiling is not always available. Therefore, surrogate immunohistochemical classifications based on estrogen receptor (ER), progesterone receptor (PR), and/or human epidermal growth factor type 2 (HER2) expression statuses are used more widely (3). Currently, the commonly accepted molecular subtypes based on expression of these receptors are luminal A, luminal B, HER2-positive, and triple-negative (4).

In breast cancer, HER2 overexpression is associated with aggressive histological features and a poor prognosis (5). However, a previous report demonstrated that patients with HER2-positive breast cancer could achieve a high pathological complete response rate following trastuzumab-containing neoadjuvant chemotherapy (6, 7). An accurate molecular subtype diagnosis is therefore needed for the development of rational, individualized treatments.

Fluorine-18 fluorodeoxyglucose (F-18 FDG)-positron emission tomography/computed tomography (PET/CT) is widely used in most malignancy workups, including detection, differential diagnosis, staging and/or restaging, therapeutic decision-making, follow-up, and prognosis (8, 9). In breast cancer, FDG uptake has been found to correlate with tumor size, histological grade, proliferation index, and molecular subtype (10-13). However, very few studies have investigated the diagnostic performance of F-18 FDG-PET/CT-based predictions of molecular subtype.

2. Objectives

The aim of this study was to evaluate the usefulness of F-18 FDG-PET/CT for the prediction of breast cancer molecular subtype.

3. Patients and Methods

3.1. Patients

This retrospective study was approved by our institutional review board, and the requirement for written

informed consent was waived. Ninety-nine consecutive patients with pathologically proven invasive breast carcinoma (IBC) underwent F-18 FDG-PET/CT imaging for pre-operative tumor staging between January 2013 and October 2014. Thirty-three of the 99 patients were excluded from our cohort study because of the post-neoadjuvant chemotherapy status ($n = 32$) or post-splenectomy status ($n = 1$). The remaining 66 patients [mean age (\pm standard deviation), 58 ± 14.6 years; age range, 27 - 86 years] with 69 IBCs were included in our study. The interval between pathological diagnosis and subsequent F-18 FDG-PET/CT evaluation ranged from 1 to 75 days (mean, 22.0 ± 1.7 days).

3.2. F-18 FDG-PET/CT Imaging

Patients were instructed to fast for at least 5 hours prior to F-18 FDG-PET/CT acquisition. Blood glucose levels were measured before scanning and were < 200 mg/dL in all patients. All imaging was performed on a 16-section PET/CT scanner (Biograph Sensation 16; Siemens Medical Solutions, Erlangen, Germany) that comprised a 16-section high-performance multi-detector low CT scanner with a lutetium oxyortho-silicate-based PET scanner. Sixty minutes after the administration of F-18 FDG (mean dose, 3.9 ± 0.7 MBq/kg; range, 2.7 - 5.9 MBq/kg), whole-body CT (from vertex to pelvis) was initially performed primarily for attenuation correction during breath-holding in the mid-expiration phase. The CT parameters were as follows: section width, 5 mm; table feed per rotation, 18 mm; rotation time, 0.5 seconds; tube voltage, 120 kVp; quality referenced mAs, 100 mAs in CARE Dose 4D; and field of view, 70 cm. Images were acquired for 2 minutes at each of eight bed positions (16.2 cm of axial field of view). Attenuation-corrected PET images were reconstructed from the CT data using a 3-D ordered subset expectation maximization algorithm (8 subsets, 3 iterations).

3.3. PET Image Analysis

A nuclear medicine physician (with 5 years of experience in the interpretation of PET images) who was unaware of the patients' clinical information retrospectively reviewed all F-18 FDG-PET/CT images on a commercially-available dedicated digital imaging and communications in medicine (DICOM) viewer. The nuclear medicine physician measured the maximum standardized uptake value of the IBC (tumor SUV_{max}) by drawing a region-of-interest (ROI) that encompassed as much of the tumor area as possible. The tumor SUV_{max} was measured on axial images over the most intense area of F-18 FDG accumulation. Additionally, an elliptical ROI was drawn to encompass as much of the right hepatic lobe as possible on the axial images to

measure the mean SUV of the liver. The mean SUV of the spleen was measured similarly. The tumor-to-liver SUV and tumor-to-spleen SUV ratios were calculated as ratios of the tumor SUV_{max} to the mean liver and spleen SUVs, respectively.

3.4. Histopathologic Analysis

ER, PR, and HER2 statuses were determined from the pathologic reports obtained during surgery ($n = 56$) or biopsy ($n = 13$). ER and PR statuses were considered positive if the Allred scores from immunohistochemical staining were ≥ 3 (14). The HER2 status was considered positive if the immunohistochemical stain score was 3+, or 2+ with fluorescence in situ hybridization (FISH)-proven HER2 gene amplification (15). IBCs were classified into four molecular subtypes according to the ER, PR, and HER2 status as follows (16): luminal A (ER positive and/or PR positive, HER2 negative), luminal B (ER positive and/or PR positive, HER2 positive), HER2-positive (ER negative, PR negative, and HER2 positive), and triple-negative (ER negative, PR negative, and HER2 negative).

3.5. Statistical Analysis

Statistical analyses were performed using MedCalc Software for Windows (version 14.12; MedCalc Software, Ostend, Belgium). The Kruskal-Wallis test was used to evaluate differences between the molecular subtypes in patient age, tumor size, mean SUVs of the liver and spleen, tumor SUV_{max}, tumor-to-liver SUV ratio, and tumor-to-spleen SUV ratio. When the Kruskal-Wallis test indicated a significant difference among the 4 molecular subtypes ($P < 0.05$), pairwise comparisons were performed using the Mann-Whitney test and a stricter P value < 0.0083 , determined using the Bonferroni correction, was considered significant.

A stepwise logistic regression analysis was performed to detect each molecular subtype using the following parameters: tumor size, tumor SUV_{max}, tumor-to-liver SUV ratio, and tumor-to-spleen SUV ratio. In this analysis, molecular subtype was considered a binary variable with a value of 1 if an IBC belonged to the molecular subtype of interest and 0 if it belonged to any other molecular subtype.

An optimal cutoff value based on maximal sensitivity and specificity was identified for the detection of each molecular subtype, using the highest area under the receiver operating characteristic (ROC) curve. ROC curves were fitted to the cutoff value to compute the sensitivity, specificity, and area under the ROC curve (AUC) for the detection of each molecular subtype. We defined significance as a P value of less than 0.05.

A post-hoc power analysis was conducted to assess our statistical power by using commercially available software (G*Power, version 3.1.7; University of Duesseldorf, Duesseldorf, Germany) with an effect size of 0.25, a significance level of 5%, and a total sample size of 66 patients.

4. Results

4.1. Patient Background Factors and Tumor Characteristics

The patients' background factors and tumor characteristics are summarized in Table 1. No significant differences in patient age ($P = 0.60$) were found between the four molecular subtypes. The 69 IBCs were classified according to molecular subtype as follows: luminal A, 53 (77%); luminal B, 6 (9%); HER2-positive, 6 (9%); and triple-negative, 4 (5%). The maximal IBC diameters ranged from 5 to 50 mm, with a mean of 19.3 ± 9.9 mm. The Kruskal-Wallis test detected a significant difference in tumor size ($P = 0.002$), although no significant differences were observed for the following pairwise comparisons conducted using the Mann-Whitney test with Bonferroni correction: $P = 0.095$ for luminal A versus luminal B, $P = 0.0087$ for luminal A versus HER2-positive, $P = 0.0090$ for luminal A versus triple-negative, $P = 0.30$ for luminal B versus HER2-positive, $P = 0.20$ for luminal B versus triple-negative, and $P = 0.75$ for luminal B versus HER2-positive.

4.2. Correlation Between SUV and Molecular Subtype

The mean SUVs of the liver and spleen, tumor SUVmax, tumor-to-liver SUV ratio, and tumor-to-spleen SUV ratio are summarized in Table 2. The mean tumor SUVmax ($P = 0.0032$), tumor-to-liver SUV ratio ($P = 0.0036$), and tumor-to-spleen SUV ratio ($P = 0.0054$) of the HER2-positive subtype were significantly greater than the corresponding values of the luminal A subtype (Figure 1). No significant differences were observed for the other pairwise comparisons ($P = 0.016 - 0.98$).

The tumor-to-liver SUV ratio correlated independently with the HER2-positive subtype ($P = 0.0049$), whereas no correlations were observed between independent factors and other subtypes. Therefore, we focused our detailed analysis on the relationship between the tumor-to-liver SUV ratio and the HER2-positive subtype.

The sensitivity and specificity of the tumor-to-liver SUV ratio for detection of the HER2-positive subtype were 83% and 79%, respectively, when employing a cutoff value of 2.33. The AUC for detection of the HER2-positive subtype was 0.87 (95% confidence interval (CI), 0.76 - 0.94) when using the tumor-to-liver SUV ratio (Figure 2). Representative F-18 FDG-PET/CT and magnetic resonance (MR) images

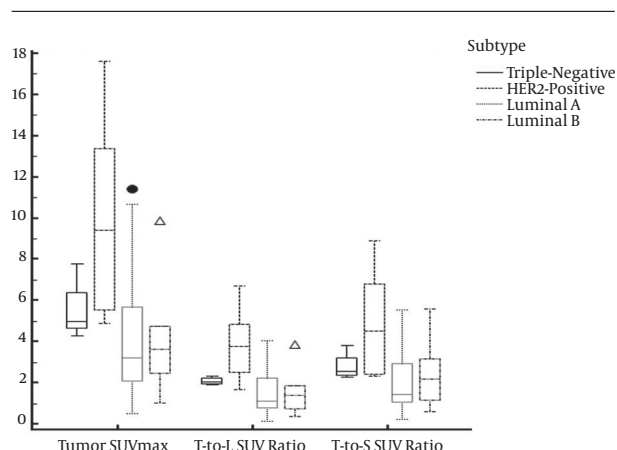


Figure 1. Box plot indicating the tumor maximum standard uptake value (SUVmax) and tumor-to-liver and spleen SUV ratios for four molecular subtypes. The mean tumor-to-liver SUV ratio was greater for the HER2-positive subtype than for the luminal A subtype ($P = 0.0036$). The boundaries of the boxes closest to zero represent the 25th percentiles, lines in the boxes indicate the medians, boundaries of boxes farthest from zero represent the 75th percentiles, the error bars denote the smallest and largest values of 1.5 box lengths of the 25th and 75th percentiles, and dots indicate the outliers.

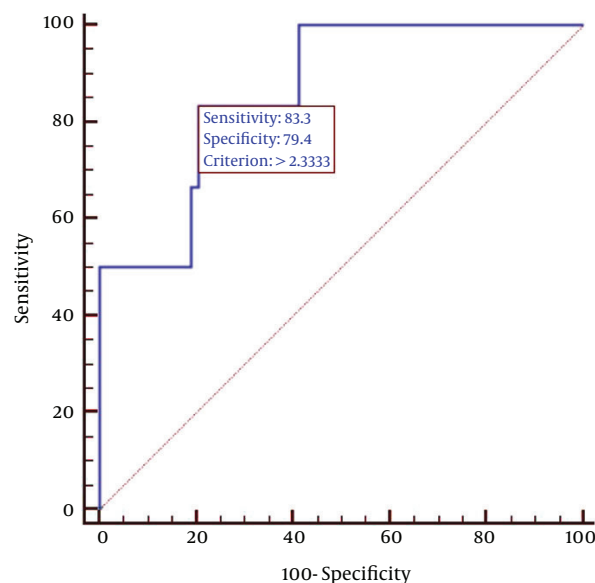


Figure 2. Receiver operating characteristic curve for detection of HER2-positive subtype. The area under the curve (AUC) for the detection of the HER2-positive subtype using the tumor-to-liver standard uptake value (SUV) ratio was 0.87.

of HER2-positive and triple-negative subtype tumors are illustrated in Figures 3 and 4, respectively. Our sample size of 66 patients was sufficient to show a 5% difference with a 35% power.

Table 1. Patient Background Factors and Tumor Characteristics^a

	Luminal A	Luminal B	HER2-Positive	Triple-Negative	P Value
No. of patients	50	6	6	4	
No. of lesions	53	6	6	4	
Age, y	58 ± 14.0 (27 - 83)	55 ± 21.2 (33 - 86)	65 ± 9.9 (48 - 78)	58 ± 10.0 (33 - 82)	0.60
Tumor size, mm	17.1 ± 9.0 (5 - 46)	21.3 ± 6.6 (10 - 27)	28.5 ± 11.9 (17 - 50)	30.8 ± 9.9 (23 - 45)	0.002 ^b

Abbreviation: HER2, human epidermal growth factor type 2.

^aPatient age and tumor size are means ± 1 standard deviation with ranges in parentheses.

^bThe Kruskal-Wallis test indicated a significant difference, but the following pairwise comparisons using the Mann-Whitney test and Bonferroni correction showed no significant difference between the four molecular subtypes.

Table 2. SUVmean of the Liver and Spleen, Tumor SUVmax, Tumor-to-Liver SUV Ratio, and Tumor-to-Spleen SUV Ratio of the Four Molecular Subtypes^a

	Luminal A (n = 53)	Luminal B (n = 6)	HER2-Positive (n = 6)	Triple-Negative (n = 4)	P Value
SUVmean of the liver	2.8 ± 0.5 (2.0 - 4.2)	2.7 ± 0.3 (2.5 - 3.3)	2.6 ± 0.3 (2.2 - 2.9)	2.6 ± 0.5 (2.2 - 3.3)	0.76
SUVmean of the spleen	2.1 ± 0.4 (1.3 - 3.3)	1.8 ± 0.1 (1.7 - 2.0)	2.1 ± 0.2 (1.9 - 2.3)	2.0 ± 0.1 (1.9 - 2.0)	0.14
Tumor SUVmax	4.4 ± 3.0 (0.5 - 11.4)	4.2 ± 3.0 (1.0 - 9.9)	10.1 ± 4.9 ^b (4.9 - 17.6)	5.5 ± 0.8 (4.3 - 7.8)	0.013
Tumor-to-liver SUV ratio	1.6 ± 1.1 (0.2 - 4.1)	1.6 ± 1.2 (0.4 - 3.9)	3.9 ± 1.9 ^b (1.7 - 6.7)	2.1 ± 0.2 (1.9 - 2.3)	0.012
Tumor-to-spleen SUV ratio	2.2 ± 1.5 (0.2 - 5.5)	2.4 ± 1.9 (0.6 - 5.6)	4.9 ± 2.6 ^b (2.3 - 8.9)	2.8 ± 0.7 (2.3 - 3.8)	0.02

Abbreviation: HER2, human epidermal growth factor type 2; SUV, standardized uptake value.

^aValues are expressed as means ± 1 standard deviation with ranges in parentheses.

^bValue was significantly greater ($P < 0.0083$) than those with luminal A by the Mann-Whitney test and Bonferroni correction.

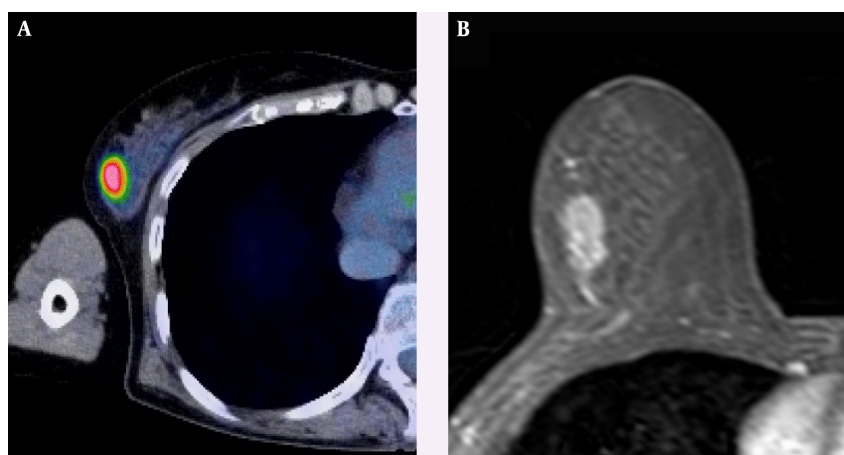


Figure 3. A 63-year-old woman with HER2-positive subtype breast cancer. A, Axial F-18 positron emission tomography/computed tomography (PET/CT) and B, Dynamic contrast-enhanced MR images show intense Fluorine-18 fluorodeoxyglucose (F-18 FDG) uptake (tumor maximum standard uptake value (SUVmax): 8.25, and tumor-to-liver SUV ratio: 2.93) in a 17-mm right breast mass confirmed to be an invasive ductal carcinoma.

5. Discussion

The local recurrence and distant metastasis rates and mortality rate are higher among patients with HER2-positive and triple-negative subtype tumors, compared to those with luminal A and B subtype tumors (17). Previous studies have correlated F-18 FDG uptake with histopatho-

logic grade, tumor size, and the hormonal receptor expression status, all of which are important prognostic factors for the long-term survival of patients with breast cancer (18-20). Notably, HER2-positive and triple-negative subtype tumors have a significantly higher mean SUVmax, compared with luminal A and B subtype tumors (21).

In a previous study, the mean SUVmax of triple-

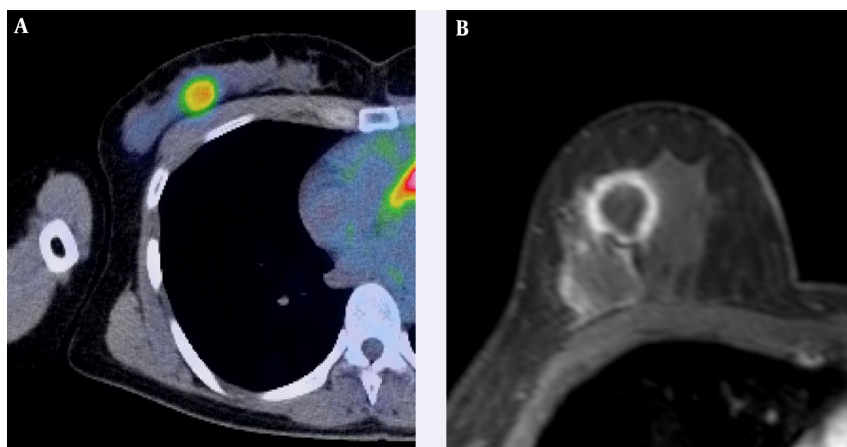


Figure 4. A 52-year-old woman with triple-negative subtype breast cancer. A, Axial F-18 positron emission tomography/computed tomography (PET/CT) and B, Dynamic contrast-enhanced MR images show intense Fluorine-18 fluorodeoxyglucose (F-18 FDG) uptake (tumor maximum standard uptake value (SUVmax): 4.31, tumor-to-liver SUV ratio: 1.93) in a 25-mm right breast mass that was confirmed as an invasive ductal carcinoma.

negative subtype tumors was greater than that of HER2-positive subtype tumors (22). However, in our study, the mean tumor-to-liver SUV ratio of HER2-positive subtype tumors was significantly greater than that of luminal A subtype tumors and greater than those of other subtypes, although those differences were not significant. On dynamic contrast-enhanced MR imaging, triple-negative subtype tumors tend to exhibit rim enhancement. The presence of a fibrotic focus in the center of an invasive breast cancer, regardless of necrosis, is associated with tumor metastasis and mortality (23, 24). In our study population, we included four patients with triple-negative subtype tumors. Of these four patients, three (75%) exhibited rim enhancement on dynamic contrast-enhanced MR imaging. We believed that the SUV of triple-negative subtype tumors with a fibrotic focus, regardless of necrosis, might be lower than that of HER2-positive subtype tumors.

In our study, we used the tumor-to-liver SUV and tumor-to-spleen SUV ratios in addition to the tumor SUVmax. The liver and spleen represent organs with high reticuloendothelial system activity. Reticuloendothelial system cells, including phagocytic cells, primary macrophages, and Kupffer cells phagocytose and thus remove dying cells, debris, and malignant cells (25). The mean SUVs of the liver and spleen tend to be greater in patients with viable malignant tumors (26). In our study, the mean liver SUV was slightly lower among HER2-positive and triple-negative subtype tumors than among luminal A and B subtype tumors, although this difference was not significant. According to a stepwise logistic regression analysis, although tumor SUVmax was not a significant parameter with regard to the discrimination of each molecular

subtype, the tumor-to-liver SUV ratio correlated independently with the HER2-positive subtype. Notably, the use of the tumor SUVmax alone led to a considerable overlap among the four subtypes.

Our study had several limitations. First, this was a retrospective study with a relatively small sample size, which might have potentially caused selection bias because a post hoc power analysis showed a power of 35%. Further clinical studies involving larger sample sizes may be needed to validate our preliminary results. Second, we included small tumors in our study. The SUVmax of a small tumor may be underestimated because of the partial volume effect (27). In our study, however, all IBCs exhibited positive F-18 FDG uptake, regardless of tumor size. Finally, we only evaluated F-18 FDG uptake when detecting each molecular subtype. However, other prognostic factors, including clinical stage, axillary lymph node involvement, distant metastasis, histologic grade, and nuclear grade, might also contribute to the wide variability in the outcomes of patients with IBCs.

In summary, our study demonstrated a significant correlation between the tumor-to-liver SUV ratio and HER2-positive subtype breast cancer. The tumor-to-liver SUV ratio appears to be a valuable index for identifying the HER2-positive subtype, thus supporting the potential of F-18 FDG-PET/CT as an imaging biomarker that could help to guide the clinical management of patients with breast cancer.

Footnotes

Authors' Contributions: Each author has equally contributed to this manuscript.

Financial Disclosure: Authors have no financial interests or conflicts.

References

- Fernandez-Morales LA, Segui MA, Andreu X, Dalmau E, Saez A, Pericay C, et al. Analysis of the pathologic response to primary chemotherapy in patients with locally advanced breast cancer grouped according to estrogen receptor, progesterone receptor, and HER2 status. *Clin Breast Cancer*. 2007;7(7):559-64. doi: [10.3816/CBC.2007.n.012](#). [PubMed: [17509165](#)].
- Tran B, Bedard PL. Luminal-B breast cancer and novel therapeutic targets. *Breast Cancer Res*. 2011;13(6):221. doi: [10.1186/bcr2904](#). [PubMed: [22217398](#)].
- Hugh J, Hanson J, Cheang MC, Nielsen TO, Perou CM, Dumontet C, et al. Breast cancer subtypes and response to docetaxel in node-positive breast cancer: use of an immunohistochemical definition in the BCIRG 001 trial. *J Clin Oncol*. 2009;27(8):1168-76. doi: [10.1200/JCO.2008.18.1024](#). [PubMed: [19204205](#)].
- Lam SW, Jimenez CR, Boven E. Breast cancer classification by proteomic technologies: current state of knowledge. *Cancer Treat Rev*. 2014;40(1):129-38. doi: [10.1016/j.ctrv.2013.06.006](#). [PubMed: [23891266](#)].
- Ross JS, Fletcher JA. HER-2/neu (c-erb-B2) gene and protein in breast cancer. *Am J Clin Pathol*. 1999;112(1 Suppl 1):S53-67. [PubMed: [10396301](#)].
- Buzdar AU, Ibrahim NK, Francis D, Booser DJ, Thomas ES, Theriault RL, et al. Significantly higher pathologic complete remission rate after neoadjuvant therapy with trastuzumab, paclitaxel, and epirubicin chemotherapy: results of a randomized trial in human epidermal growth factor receptor 2-positive operable breast cancer. *J Clin Oncol*. 2005;23(16):3676-85. doi: [10.1200/JCO.2005.07.032](#). [PubMed: [15738535](#)].
- Untch M, Fasching PA, Konecny GE, Hasmuller S, Lebeau A, Kreienberg R, et al. Pathologic complete response after neoadjuvant chemotherapy plus trastuzumab predicts favorable survival in human epidermal growth factor receptor 2-overexpressing breast cancer: results from the TECHNO trial of the AGO and GBG study groups. *J Clin Oncol*. 2011;29(25):3351-7. doi: [10.1200/JCO.2010.31.4930](#). [PubMed: [21788566](#)].
- Hustinx R, Benard F, Alavi A. Whole-body FDG-PET imaging in the management of patients with cancer. *Semin Nucl Med*. 2002;32(1):35-46. doi: [10.1053/snuc.2002.29272](#). [PubMed: [11839068](#)].
- Scott AM. Current status of positron emission tomography in oncology. *Intern Med J*. 2001;31(1):27-36. [PubMed: [11478353](#)].
- Bos R, van Der Hoeven JJ, van Der Wall E, van Der Groep P, van Diest PJ, Comans EF, et al. Biologic correlates of (18)fluorodeoxyglucose uptake in human breast cancer measured by positron emission tomography. *J Clin Oncol*. 2002;20(2):379-87. doi: [10.1200/JCO.2002.20.2.379](#). [PubMed: [11786564](#)].
- Groheux D, Giacchetti S, Moretti JL, Porcher R, Espie M, Lehmann-Che J, et al. Correlation of high 18F-FDG uptake to clinical, pathological and biological prognostic factors in breast cancer. *Eur J Nucl Med Mol Imaging*. 2011;38(3):426-35. doi: [10.1007/s00259-010-1640-9](#). [PubMed: [21057787](#)].
- Buck A, Schirrmeyer H, Kuhn T, Shen C, Kalker T, Kotzerke J, et al. FDG uptake in breast cancer: correlation with biological and clinical prognostic parameters. *Eur J Nucl Med Mol Imaging*. 2002;29(10):1317-23. doi: [10.1007/s00259-002-0880-8](#). [PubMed: [12271413](#)].
- Osborne JR, Port E, Gonen M, Doane A, Yeung H, Gerald W, et al. 18F-FDG PET of locally invasive breast cancer and association of estrogen receptor status with standardized uptake value: microarray and immunohistochemical analysis. *J Nucl Med*. 2010;51(4):543-50. doi: [10.2967/jnumed.108.060459](#). [PubMed: [20237034](#)].
- Allred DC, Harvey JM, Berardo M, Clark GM. Prognostic and predictive factors in breast cancer by immunohistochemical analysis. *Modern Pathol Official J United States Can Acad Pathol*. 1998;11(2):155-68.
- Perez EA, Roche PC, Jenkins RB, Reynolds CA, Halling KC, Ingle JN, et al. HER2 testing in patients with breast cancer: poor correlation between weak positivity by immunohistochemistry and gene amplification by fluorescence in situ hybridization. *Mayo Clin Proc*. 2002;77(2):148-54. doi: [10.4065/77.2.148](#). [PubMed: [11838648](#)].
- Huber KE, Carey LA, Wazer DE. Breast cancer molecular subtypes in patients with locally advanced disease: impact on prognosis, patterns of recurrence, and response to therapy. *Semin Radiat Oncol*. 2009;19(4):204-10. doi: [10.1016/j.semradonc.2009.05.004](#). [PubMed: [19732684](#)].
- Garcia Fernandez A, Chabrera C, Garcia Font M, Fraile M, Lain JM, Gonzalez S. Differential patterns of recurrence and specific survival between luminal A and luminal B breast cancer according to recent changes in the 2013 St Gallen immunohistochemical classification. Clinical & translational oncology. Official publication of the Federation of Spanish Oncology Societies and of the National Cancer Institute of Mexico; 2014.
- Koolen BB, Vrancken Peeters MJ, Wesseling J, Lips EH, Vogel WV, Aukema TS, et al. Association of primary tumour FDG uptake with clinical, histopathological and molecular characteristics in breast cancer patients scheduled for neoadjuvant chemotherapy. *Eur J Nucl Med Mol Imaging*. 2012;39(12):1830-8. doi: [10.1007/s00259-012-2211-z](#). [PubMed: [22895862](#)].
- Koolen BB, Pengel KE, Wesseling J, Vogel WV, Vrancken Peeters MJ, Vincent AD, et al. FDG PET/CT during neoadjuvant chemotherapy may predict response in ER-positive/HER2-negative and triple negative, but not in HER2-positive breast cancer. *Breast*. 2013;22(5):691-7. doi: [10.1016/j.breast.2012.12.020](#). [PubMed: [23414930](#)].
- Kumar R, Chauhan A, Zhuang H, Chandra P, Schnell M, Alavi A. Clinicopathologic factors associated with false negative FDG-PET in primary breast cancer. *Breast Cancer Res Treat*. 2006;98(3):267-74. doi: [10.1007/s10549-006-9159-2](#). [PubMed: [16555126](#)].
- Koo HR, Park JS, Kang KW, Cho N, Chang JM, Bae MS, et al. 18F-FDG uptake in breast cancer correlates with immunohistochemically defined subtypes. *Eur Radiol*. 2014;24(3):610-8. doi: [10.1007/s00330-013-3037-1](#). [PubMed: [24097303](#)].
- Jo JE, Kim JY, Lee SH, Kim S, Kang T. Preoperative 18F-FDG PET/CT predicts disease-free survival in patients with primary invasive ductal breast cancer. *Acta Radiol*. 2015;56(12):1463-70. doi: [10.1177/0284185114556929](#). [PubMed: [25406431](#)].
- Hasebe T, Tsuda H, Hirohashi S, Shimosato Y, Tsubono Y, Yamamoto H, et al. Fibrotic focus in infiltrating ductal carcinoma of the breast: a significant histopathological prognostic parameter for predicting the long-term survival of the patients. *Breast Cancer Res Treat*. 1998;49(3):195-208. [PubMed: [9776503](#)].
- Van den Eynden GG, Smid M, Van Laere SJ, Colpaert CG, Van der Auwera I, Bich TX, et al. Gene expression profiles associated with the presence of a fibrotic focus and the growth pattern in lymph node-negative breast cancer. *Clin Cancer Res*. 2008;14(10):2944-52. doi: [10.1158/1078-0432.CCR-07-4397](#). [PubMed: [18483361](#)].
- Parkin J, Cohen B. An overview of the immune system. *Lancet*. 2001;357(9270):1777-89. doi: [10.1016/S0140-6736\(00\)04904-7](#). [PubMed: [11403834](#)].
- Bural GG, Torigian DA, Chen W, Houseni M, Basu S, Alavi A. Increased 18F-FDG uptake within the reticuloendothelial system in patients with active lung cancer on PET imaging may indicate activation of the systemic immune response. *Hell J Nucl Med*. 2010;13(1):23-5. [PubMed: [2041166](#)].
- Soret M, Bacharach SL, Buvat I. Partial-volume effect in PET tumor imaging. *J Nucl Med*. 2007;48(6):932-45. doi: [10.2967/jnumed.106.035774](#). [PubMed: [17504879](#)].